Molecular Biology of the Cell
Vol. 14, 3156–3168, August 2003

Differential Caveolin-1 Polarization in Endothelial Cells during Migration in Two and Three Dimensions

Marie-Odile Parat,* Bela Anand-Apte,† and Paul L. Fox*‡

*Department of Cell Biology, The Lerner Research Institute, Cleveland Clinic Foundation, Cleveland, Ohio 44195; and †Cole Eye Institute, Cleveland Clinic Foundation, Cleveland, Ohio 44195

Submitted November 22, 2002; Revised March 27, 2003; Accepted April 17, 2003
Monitoring Editor: Anthony Bretscher

Endothelial cell (EC) migration is a critical event during multiple physiological and pathological processes. ECs move in the plane of the endothelium to heal superficially injured blood vessels but migrate in three dimensions during angiogenesis. We herein investigate differences in these modes of movement focusing on caveolae and their defining protein caveolin-1. Using a novel approach for morphological analysis of transmigrating cells, we show that ECs exhibit a polarized distribution of caveolin-1 when traversing a filter pore. Strikingly, in these cells caveolin-1 seems to be released from caveolar structures in the cell rear and to relocalize at the cell front in a cytoplasmic form. In contrast, during planar movement caveolin-1 is concentrated at the rear of ECs, colocalizing with caveolae. The phosphorylatable Tyr^{14} residue of caveolin-1 is required for polarization of the protein during transmigration but does not alter polarization during planar movement. Palmitoylation of caveolin-1 is not essential for redistribution of the protein during either mode of movement. Thus, ECs migrating in three dimensions uniquely exhibit dissociation of caveolin-1 from caveolae and phosphorylation-dependent relocalization to the cell front.

INTRODUCTION

Endothelial cell (EC) migration is an essential component of vasculogenesis and angiogenesis, processes by which new blood vessels are created or capillaries are formed from preexisting blood vessels, respectively (Anand-Apte and Fox, 2002). EC migration is also a critical step in the regeneration of the endothelium after arterial injury (Haudenschild and Schwartz, 1979). The topology of EC movement during these events differs significantly, namely, blood vessel formation is a three-dimensional process in which ECs exit the plane of the endothelium, whereas wound healing is a two-dimensional process in which ECs remain within this plane. EC locomotion on flat surfaces in vitro is similar to that of fibroblasts and other crawling cells and is characterized by a spatially polarized series of events: protrusion of a lamellipodium and filopodia at the leading edge, attachment to the substratum, forward flow of cytosol, and focal adhesion loosening and tail retraction at the rear of the cell. Intracellular, motility-related structures and processes also exhibit anterior-posterior polarization in crawling cells, including integrin-cytoskeleton interactions (Schmidt *et al.*, 1993); actin polymerization/depolymerization; and translocation of multiple motor, regulatory, and signaling molecules (Kolega, 1998; Lawrence and Singer, 1986). Much less is known about the polarization of cellular structures during three-dimensional migration through pores, possibly because of methodological difficulties imposed by the experimental system.

Caveolae are cave-like invaginations at the surface of multiple cell types and are particularly abundant in vascular ECs (Simionescu *et al.*, 1982; Lisanti *et al.*, 1994). They are specialized membrane subdomains rich in glycosphingolipids and cholesterol and also in lipid-anchored membrane proteins. The major protein component of caveolae is caveolin-1, an integral membrane protein with an unusual hairpin-like conformation in which the N- and C-terminal regions both face the cytosol and are connected by a membrane-embedded, hydrophobic domain (Dupree *et al.*, 1993). Caveolin-1 is found as two major isoforms, caveolin-1α and -1β, derived from alternate translation-initiation sites of the same transcript; the smaller β-isoform lacks 31 amino acids at the N terminus (Scherer *et al.*, 1995). Caveolin-1 participates in multiple protein–protein and protein–lipid interactions that are critical for its diverse functions. Caveolin-1 is subject to two types of posttranslational modifications that regulate its intracellular localization or activity, namely, phosphorylation and palmitoylation. Several stimuli, including oxidative stress, induce phosphorylation of caveolin-1α on Tyr^{14} (Volonte *et al.*, 2001; Parat *et al.*, 2002;

Article published online ahead of print. Mol. Biol. Cell 10.1091/mbc.E02–11–0761. Article and publication date are available at www.molbiolcell.org/cgi/doi/10.1091/mbc.E02–11–0761.

‡ Corresponding author. E-mail address: foxp@ccf.org.

Abbreviations used: BSA, bovine serum albumin; EC, endothelial cell; FGF, fibroblast growth factor; GFP, green fluorescent protein; PBS, phosphate-buffered saline.

Sanguinetti and Mastick, 2003). Like many caveolae-targeted proteins, caveolin-1 is acylated; three Cys residues near the C termini (of both α- and β-isoforms) are susceptible to palmitoylation (Dietzen *et al.*, 1995). Palmitoylation is not required for caveolin-1 targeting to caveolae (Dietzen *et al.*, 1995; Uittenbogaard and Smart, 2000), but mutation of the Cys residues impairs caveolin-1 interaction with other acylated proteins (Lee *et al.*, 2001) and its binding and transport of cholesterol (Uittenbogaard and Smart, 2000).

Caveolin-1 may have an important role in cell motility because it exhibits anterior-posterior polarization during cell migration. Caveolin-1 was reported to accumulate at the leading edge of cultured fibroblasts (Rothberg *et al.*, 1992), human umbilical vein smooth muscle cells (Okada *et al.*, 1995), and caveolin-deficient FRT cells expressing recombinant caveolin-1 (Scherer *et al.*, 1995). In contrast, caveolin-1 accumulated in the trailing edge of bovine aortic ECs (Isshiki *et al.*, 2002). Caveolae or lipid rafts also exhibit pronounced polarity during cell migration. Raft-associated ganglioside GM1 was found at the leading edge of human adenocarcinoma MCF-7 cells stimulated with insulin growth factor-1 (Mañes *et al.*, 1999). Cholesterol depletion disrupted raft formation and cellular acquisition of polarity, indicating a functional role of the rafts and that raft movement to the front of the cell may be critical for polarization of motility-related, raft-associated proteins. The same laboratory subsequently reported that ganglioside GM1 was in the *rear* of a moving T lymphocyte (Gómez-Moutón *et al.*, 2001). Herein, we investigate the polarization of caveolin-1 and caveolae in a single cell type, namely, aortic EC, during two modes of movement: two-dimensional movement in response to the wounding of a monolayer and three-dimensional movement during transmigration through a pore. We have observed differential polarization of caveolin-1 in the two migration modes and that Tyr^{14} is critical for caveolin-1 polarization only during transmigration.

MATERIALS AND METHODS

Rabbit anti-caveolin-1 and mouse anti-phosphocaveolin-1 antibodies were obtained from Transduction Laboratories (Lexington, KY). Alexa Fluor 488-phalloidin was from Molecular Probes (Eugene, OR). Biotinylated goat anti-rabbit antibody, Texas Red-avidin, and Vectashield mounting medium were from Vector Laboratories (Burlingame, CA). Gold-conjugated goat anti-rabbit IgG was purchased from Ted Pella (Redding, CA). Monoclonal anti-green fluorescent protein (GFP) antibody was from BD Biosciences Clontech (Palo Alto, CA). Basic fibroblast growth factor (FGF) was from Upstate Biotechnology (Lake Placid, NY). Rat tail collagen and all other reagents were from Sigma-Aldrich (St. Louis, MO).

Cell Culture

Bovine aortic ECs were isolated as described previously (Fox and DiCorleto, 1984) and maintained in DMEM and F12 medium supplemented with 5% fetal bovine serum, 100 U ml^{-1} penicillin, and 100 μg ml^{-1} streptomycin, in a humidified atmosphere containing 5% CO_2. In some experiments, ECs were grown on chamber slides (Falcon; BD Biosciences, Franklin Lakes, NJ).

Determination of Caveolin-1 Localization in Transmigrating ECs

A Boyden migration chamber was prepared with serum-free media alone or with 10 ng ml^{-1} of basic FGF in the lower well. Polycarbonate membranes with 8-μm pores (Neuro Probe, Gaithersburg, MD) precoated overnight with rat tail collagen type 1 (100 μg ml^{-1} in 0.2 N acetic acid) and air-dried, were used to separate the chambers. After pH equilibration of the chamber in a 5% CO_2-containing atmosphere, a suspension of 300,000 cells/ml in serum-free medium was added to the upper well, and cells were allowed to attach and migrate for 2 h. For immunofluorescence, the polycarbonate membrane was then washed in phosphate-buffered saline (PBS), fixed, permeabilized, and immunostained as described. The membranes were mounted between slide and coverslip by using mounting medium (Vectashield; Vector Laboratories) before visualization by confocal immunofluorescence microscopy. In some experiments, the membranes were cut into 0.2-cm^2 pieces and processed for electron microscopy.

Detection of Caveolin-1 in ECs by Immunofluorescence Microscopy

ECs were washed with PBS, fixed with 3.7% formaldehyde in PBS for 20 min, and then washed three times (this treatment and all subsequent treatments were done at room temperature). The cells were permeabilized with 0.1% Triton X-100 for 10 min and washed. To reduce nonspecific binding of antibody, cells were preincubated with 3% goat serum (Invitrogen, Carlsbad, CA) in PBS for 20 min. ECs were then incubated with anti-caveolin-1 polyclonal antibody (1 μg ml^{-1}) in a solution containing 1.5% goat serum in PBS for 60 min. After three washes with PBS and a 5-min incubation with 3% nonimmune goat serum, the cells were incubated with biotinylated goat anti-rabbit antibody (1:1000) in 1.5% goat serum for 45 min. After washing, cells were incubated with Texas Red-avidin (1:1000 in PBS) for 10 min, washed, and placed in Vectashield mounting medium. No reactivity was observed when the primary antibody was substituted with nonimmune rabbit IgG (1 μg ml^{-1}), or with buffer. Autofluorescence of ECs was not detectable under our experimental conditions.

Determination of Caveolin-1 Localization in Migrating ECs by Immunoelectron Microscopy

After 24 h of migration in the planar wounding assay or 2 h of migration through the pores of collagen-coated polycarbonate membranes, ECs were fixed with 4% paraformaldehyde and 0.05% glutaraldehyde in PBS at room temperature, rinsed, permeabilized with 0.7% saponin in PBS for 10 min, and washed with PBS. Cells were dehydrated on ice by using solutions from 30 to 95% ethanol containing 1 mg ml^{-1} sodium borohydrate, and rehydrated using solutions from 70 to 30% ethanol for 2 min each on ice. Cells were then washed and preincubated for 1 h in PBS containing 0.1% saponin and 1% bovine serum albumin (BSA). Cells were incubated overnight at 4°C in a humidified chamber with rabbit anti-caveolin-1 IgG or control rabbit IgG (1:500 in PBS containing 0.1% saponin and 1% BSA), washed, and placed for 30 min in a solution of 0.1% gelatin and 0.1% BSA in PBS. Cells were incubated for 1 h in 5-nm gold-conjugated goat anti-rabbit IgG (1:10) in PBS containing 0.1% gelatin and 0.1% BSA, washed, and fixed in 1.33% glutaraldehyde in 0.1 M sodium cacodylate for 20 min. Cells were rinsed in 0.1 M sodium cacodylate and incubated 5 min with 0.1 M ammonium chloride in 0.1 M sodium cacodylate. Cells were postfixed for 2 h at 4°C in 1% osmium tetraoxide containing 1.5% potassium ferricyanide. Samples were dehydrated before eponate infiltration and embedding. No gold particles could be observed when the anti-caveolin-1 IgG was replaced by nonimmune rabbit IgG.

Expression of Caveolin-1-GFP in ECs

Full-length human caveolin-1 cDNA was obtained from American Type Culture Collection (Manassas, VA) and subcloned into the EcoR1 and *Not*I sites of pcDNA3 (Invitrogen). C-Terminal-tagged caveolin-1-GFP was made by polymerase chain reaction (PCR) am-

plification of caveolin-1 from pcDNA3-caveolin-1 by using a T7 primer and 5′-CGGTACCGTTATTTCTTTCTGCAAGTTGATGCG, followed by the cloning of the *Eco*R1-*Kpn*I fragment from the PCR product into a pEGFP-N1 expression vector (BD Biosciences Clontech). The resulting construct (caveolin-1-GFP) encoded the human caveolin-1 open reading frame in-frame and upstream of the enhanced GFP sequence with a 12-amino acid spacer, all driven by a cytomegalovirus promoter. C-Terminal–tagged caveolin-1 behaves in the same way as endogenous caveolin-1, including oligomerization (Pelkmans *et al.*, 2001), whereas N-terminally tagged caveolin-1 is a dominant-negative inhibitor of simian virus 40 internalization. We also generated palmitoylation-deficient caveolin-1-GFP in which Cys^{133}, Cys^{143}, and Cys^{156} were simultaneously mutated to Ser by using 5′-AGTTGTACCATCTATTAAGAGCTTCCTGATTGAGATTCAGTCTATCAGCCGTGTCTATTCCATCTACGTCCACACCGTCTCTGACCCACT to introduce the mutations, and a phosphorylation-deficient, C-terminal GFP-tagged caveolin-1 in which Tyr^{14} was mutated to Ala (A14) by using 5′-ATGGGAACGGTGGCGAGATGTC. Caveolin-1β-GFP was generated from caveolin-1-GFP by using 5′-AACTGCAGCAAGGCCATG and 5′-CTTGCTCACCATGGTGGC as primers for PCR, and the *Pst*-1-*Bam*H1 fragment of the PCR product was cloned into pEGFP-N1. ECs were transfected using lipofectin (Invitrogen) according to the manufacturer's instructions.

Immunoblot Analysis of Phosphocaveolin-1 and Caveolin-1-GFP

ECs were washed twice in PBS and lysed at 4°C in buffer containing 50 mM HEPES, pH 7.4, 150 mM NaCl, 1 mM EDTA, 2.5 mM $MgCl_2$, 0.5% sodium deoxycholate, 1% NP-40, 20 μg ml^{-1} aprotinin, and 5 μg ml^{-1} leupeptin for 90 min. Cells were scraped, and the lysate was cleared by centrifugation at 16,000 $\times$ *g* for 3 min and added to SDS (0.1% final concentration). Anti-caveolin-1 antibody was added for 90 min, followed by protein A-Sepharose for 60 min. A control cell lysate was immunoprecipitated with rabbit nonimmune IgG. Immunoprecipitated complexes were washed three times, separated by SDS-PAGE, and transferred to nitrocellulose. Phosphocaveolin-1 was detected by immunoblot analysis with monoclonal anti-phosphocaveolin-1 as primary antibody and peroxidase-conjugated secondary antibody. Caveolin-1-GFP was detected on the same blot after stripping by using monoclonal anti-GFP primary antibody. Blots were developed by chemiluminescence with ECL and Hyperfilm-ECL (Amersham Biosciences, Piscataway, NJ).

Determination of Caveolin-1 Palmitoylation in ECs by Metabolic Labeling with [^{3}H]Palmitate

Caveolin-1 palmitoylation was measured essentially as described previously (Parat and Fox, 2001). Confluent ECs in 35-mm dishes were washed with serum-free DMEM and then incubated for 2 h in the same medium. ECs were radiolabeled for 4 h by incubation with [^{3}H]palmitic acid (250 μCi/ml) in serum-free medium containing 3.5 mg/ml fatty acid-free bovine serum albumin, and the cells lysed. Caveolin-1 and caveolin-1-GFP were immunoprecipitated using rabbit polyclonal anti-caveolin-1 antibody and subjected to SDS-PAGE as described above. Radiolabel was determined by fluorography after 1- and 6-mo exposure for endogenous caveolin-1 and for transfected caveolin-1-GFP, respectively.

RESULTS

The Vector of Caveolin-1 Polarization Depends on the Mode of EC Migration

To visualize caveolin-1 during transmigration, bovine aortic ECs were placed in the upper well of a Boyden chamber and permitted to migrate for 2 h through 8-μm pores of a collagen-coated membrane toward basic FGF placed in the lower wells. To establish that transmigrating cells could be visualized by fluorescence confocal microscopy, the membrane was fixed and actin filaments stained with fluorescently labeled phalloidin (Alexa Fluor 488-phalloidin). Cross sections (xz-planes) through the filter showed ECs on the filter surface with large protrusions extending into the pore, sometimes reaching the lower face of the filter (Figure 1A). Caveolin-1 was visualized with polyclonal rabbit anti-caveolin-1, biotinylated anti-rabbit IgG, and Texas Red-avidin. Transmigrating ECs showed abundant and polarized accumulation of caveolin-1 that was primarily restricted to the protrusion extending into the pore (Figure 1B). A series of cross-sectional views through the pore showed that caveolin-1 was not confined to the plasma membrane, but instead was distributed throughout the cytoplasm of the protrusion (Figure 1, C–E). Caveolin-1 was observed in the forward extensions of most transmigrating ECs, including those in earlier stages of transmigration with small protrusions into the pore (Figure 1, F and G). Occasionally, caveolin-1 was present in small, discrete patches decorating the rear of the cell (Figure 1B). Specificity of caveolin-1 immunostaining was established by a control in which primary anti-caveolin IgG was replaced by nonimmune rabbit IgG (Figure 1H).

Our findings seemed to be inconsistent with a recent report of caveolin-1 accumulating primarily at the trailing edge of aortic ECs induced to migrate by wounding a monolayer or by exposing cells to shear stress (Isshiki *et al.*, 2002). The apparent discrepancy may be explained by the different modes of migration in the experiments, i.e., two-dimensional movement in the wound-healing assay versus three-dimensional movement in the transmigration assay. To test whether the mode of movement was critical in determining the polarization vector, caveolin-1 was observed in cells induced to move in two dimensions by wounding an EC monolayer. Assuming that ECs move from the dense, undisturbed region of cells into the cell-free wound area, caveolin-1 seemed to concentrate in the rear of most cells (marked by arrows in Figure 2, A and B), a finding consistent with that of Isshiki *et al.* (2002). However, caveolin-1 seemed to concentrate in the front or sides of other cells (Figure 2, A and B, arrowheads). Thus, polarization may vary from cell to cell, or more likely, the perceived variability may result from an uncertainty in the direction of cell movement in a static view.

To rigorously assess the orientation of caveolin-1 polarization in ECs moving on a flat surface, time-lapse videomicroscopy was used to determine the direction of EC movement. To detect caveolin-1 in live cells, ECs were transiently transfected with a pEGFP-N1 expression vector encoding chimeric caveolin-1-GFP, and the expressed protein was detected by the green fluorescence. Colocalization of exogenous caveolin-1-GFP (Figure 2C) and cellular caveolin-1 (Figure 2D) in migrating ECs was shown in an overlay of the two images (Figure 2E). A time-lapse experiment was done in which the monolayer of transfected ECs was wounded, and fluorescent light images (Figure 2, F–J) and transmitted light images (Figure 2, K–O) of the wound edge were captured. About 6 h after wounding, caveolin-1-GFP was clearly concentrated at the rear half of an EC migrating into the cell-free area of the dish. In this and other time-lapse series, caveolin-1 polarization coincided with the generation

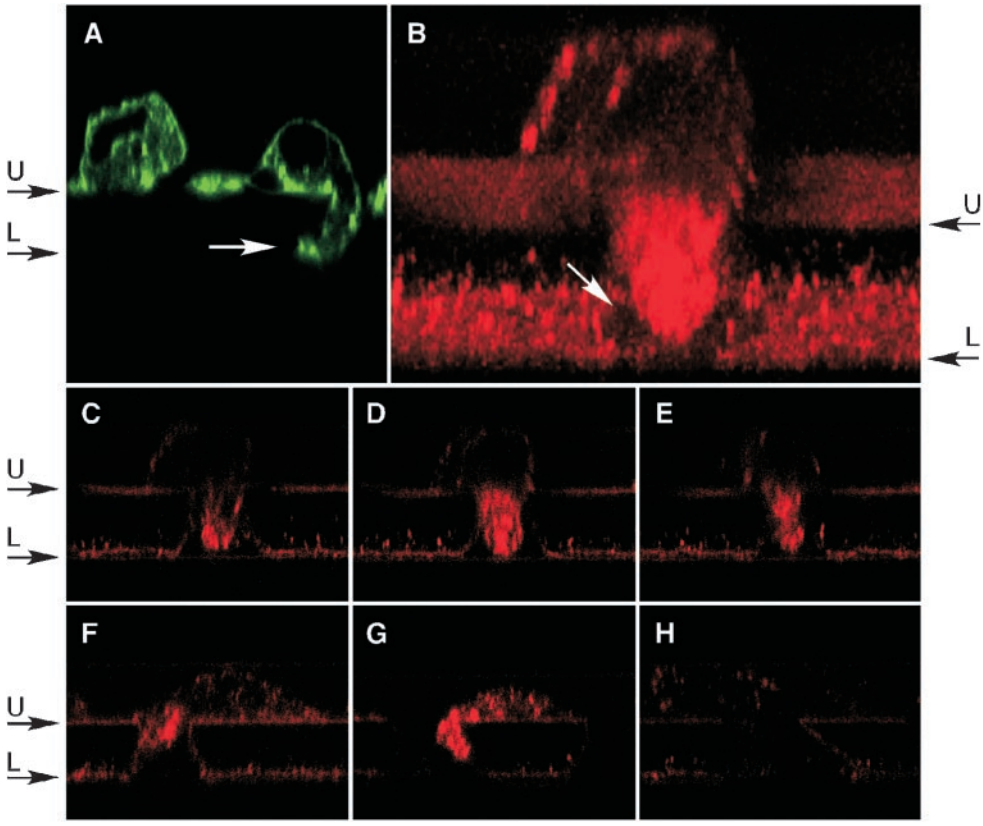

Figure 1. Caveolin-1 accumulates in the forward extension of transmigrating ECs. ECs were allowed to migrate for 2 h across a collagen-coated polycarbonate filter (8-μm pore size) toward 10 ng ml^{-1} basic FGF in the lower compartment of a Boyden chamber. The ECs were washed, fixed, stained, and imaged by fluorescence confocal microscopy in a plane through the center of the pore. (A) EC actin visualized by staining with Alexa Fluor 488-phalloidin. Cells are attached to the upper face (U) of the filter. A large cellular protrusion into a filter pore (white arrow) has reached the lower face of the filter (L). (B) Caveolin-1 was visualized by fluorescence confocal microscopy by using rabbit anti-human caveolin-1 as primary antibody followed by biotinylated goat anti-rabbit antibody and Texas Red-avidin. A three-dimensional reconstruction of caveolin-1 immunofluorescence in a transmigrating EC was generated from a series of xz-views. The front is tilted downward by 20° to facilitate visualization of the pore in the lower face of the filter (white arrow). (C–E) Individual xz-views of the cell in B at 2.25-μm intervals. (F and G) Immunofluorescence images (xz-views) of caveolin-1 in other transmigrating ECs from the same experiment. (H) Immunofluorescence image of a transmigrating cell from the same experiment, by using nonimmune, rabbit IgG instead of anti-caveolin-1 as an immunostaining control.

of morphological cell polarity. Interestingly, the fragment of cellular material that EC sometimes leave behind after tail retraction was highly enriched in caveolin-1-GFP (Figure 2, I and J). In control ECs transfected with the empty pEGFP-N1 vector, GFP was uniformly distributed throughout the cytosol, including the lamellipodium, of migrating ECs (our unpublished data). In other time-lapse images of isolated ECs, we excluded the possibility that caveolin-1 localization was influenced by cell-to-cell contacts that are primarily in the rear of cells, leaving a confluent region. For example, Figure 2, P–R, shows an isolated EC in which caveolin-1 was localized almost exclusively in the cell rear, whereas the cell moved rapidly away from the confluent region. After ~15 h, the cell stopped its forward movement and reversed direction. During the short time it took to change direction, caveolin-1 depolarized and redistributed primarily in the central region of the cell (Figure 2S). The caveolin-1 then repolarized in the opposite end of the elongated cell as it began to move in the reverse direction (Figure 2, T and U). These results indicate that the orientation of caveolin-1 polarization during two-dimensional, wound-induced migration is opposite to that observed during three-dimensional, transmigratory EC movement.

Several control experiments were done to show that the difference in caveolin-1 polarization was not due to subtle differences in culture conditions. The shift of caveolin-1 to the leading extension of a transmigrating EC was not due to the chemotactic gradient because identical polarization of caveolin-1 was observed when basic FGF was excluded from the lower well of the Boyden chamber (although fewer migrating cells were observed). We also showed that the downward movement of the transmigrating EC did not influence caveolin-1 localization because identical results were seen when the Boyden chamber was inverted. To determine whether the difference in caveolin-1 polarization was due to substrate differences in the two assays, a planar, wound-induced migration assay was done using EC on a collagen-coated polycarbonate filter (with 0.4-μm pores to prevent transmigration) as substrate. As before, caveolin-1 was preferentially localized in the rear of the EC, especially at the perimeter of the cell body and in the retracting tail (Figure 2V). A small amount of caveolin-1 is present in a punctate pattern in the forward half of the moving cell, but it is absent from the region of actin ruffling (Figure 2, W and X). Together, these results indicate that the differential polarization of caveolin-1 in the two experimental models is not due to a variant in the culture condition but rather is a function of the dissimilar modes of cell movement.

Caveolin-1 and Caveolae Do Not Colocalize in Transmigrating ECs

Caveolin-1 is an integral component of caveolar vesicles, and they generally colocalize in the cell (Schnitzer *et al.*,

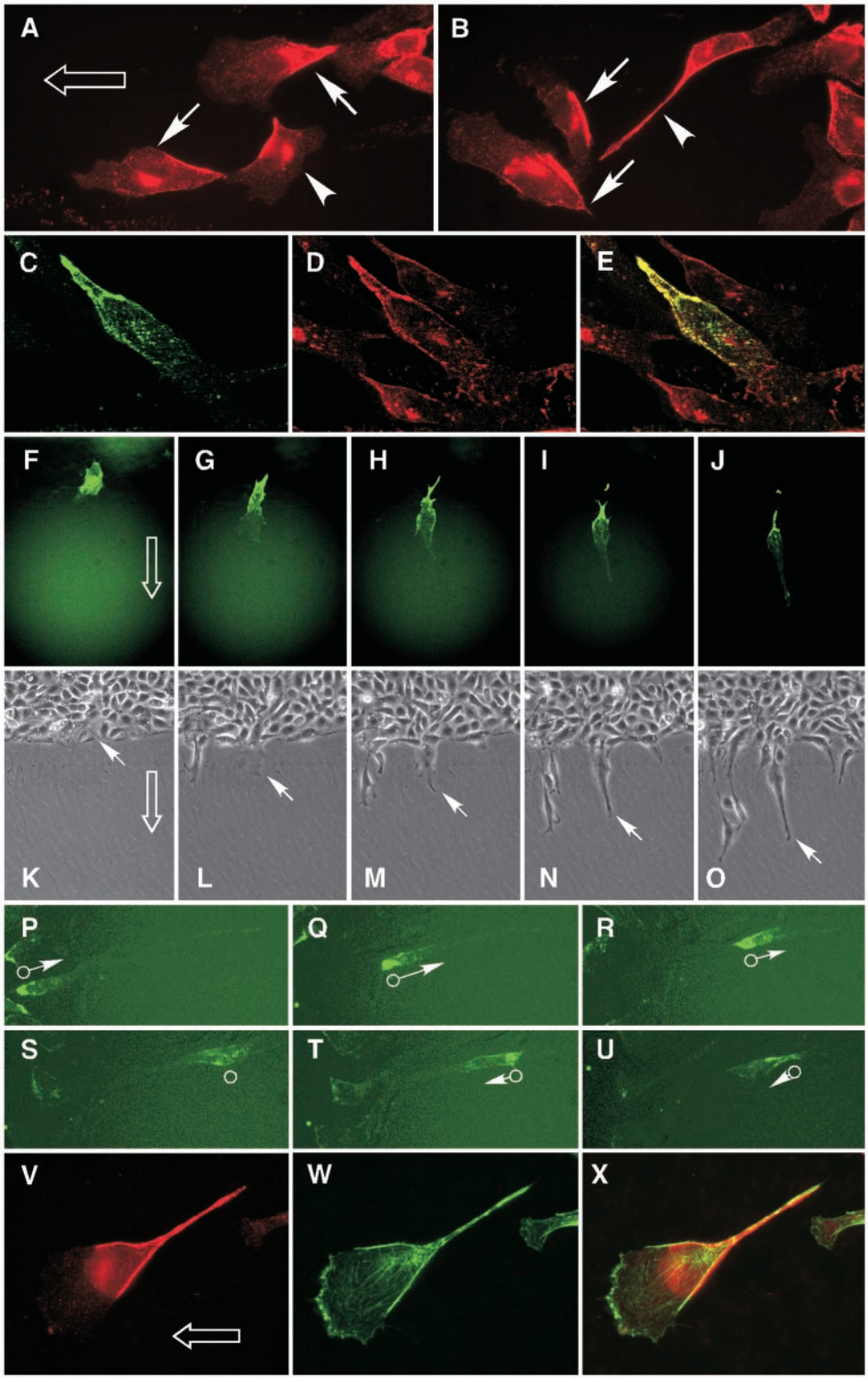

Figure 2. Caveolin-1 accumulates in the rear of planar-migrating ECs. (A and B) Confluent ECs were subjected to wound-induced planar migration for 24 h in the presence of 10 ng ml^{-1} basic FGF. The direction of overall cell migration into the wound area is indicated by an open arrow. Immunofluorescence microscopy with anti-caveolin-1 antibody shows that caveolin-1 is concentrated in the rear of most migrating cells (arrows), but a minority of cells (arrowheads) exhibit caveolin-1 in their forward regions. (C–E) ECs were transfected with a plasmid encoding caveolin-1-GFP and permitted to migrate for 24 h in the presence of 10 ng ml^{-1} basic FGF. Caveolin-1-GFP was detected by the green fluorescence of GFP (C), cellular caveolin-1 was detected by immunostaining with anti-caveolin-1 antibody and visualization with Texas Red (D), and their colocalization shown as yellow in a merged image (E). (F–O) Time-lapse video microscopy of ECs transiently transfected with caveolin-1-GFP and subjected to planar, wound-induced migration. Fluorescence microscopy images showing a single transfected EC moving into the wound area (direction indicated by open arrow) are shown 0 (F), 6.5 (G), 10 (H), 16 (I), and 24 (J) h after the wound was made. Transmitted light images of the same field and at the same times as in F–J are shown in K–O. The leading edge of the cell expressing caveolin-1-GFP is indicated by the white arrow. (P–U) ECs were transiently transfected with caveolin-1-GFP (palmitoylation-mutant; see below) and allowed to migrate under a fluorescence microscope camera and images recorded every 10 min for 24 h. Images shown were recorded after 5 h (P) and every 200 min (Q–U). The rear of the cell is indicated by the open circle, and the direction and relative velocity of the moving cell are indicated by the arrow and its length. (V–X) Aortic ECs were grown to confluence on a collagen-coated polycarbonate filter (0.4-μm pores) and induced to migrate in the presence of 10 ng ml^{-1} basic FGF on the surface of the filter by wounding the monolayer. The cells were fixed after 24 h, caveolin-1 was visualized by immunostaining (V), actin was visualized with Alexa Fluor 488-phalloidin (W), and overlay of caveolin-1 and actin was shown in the merged image (X).

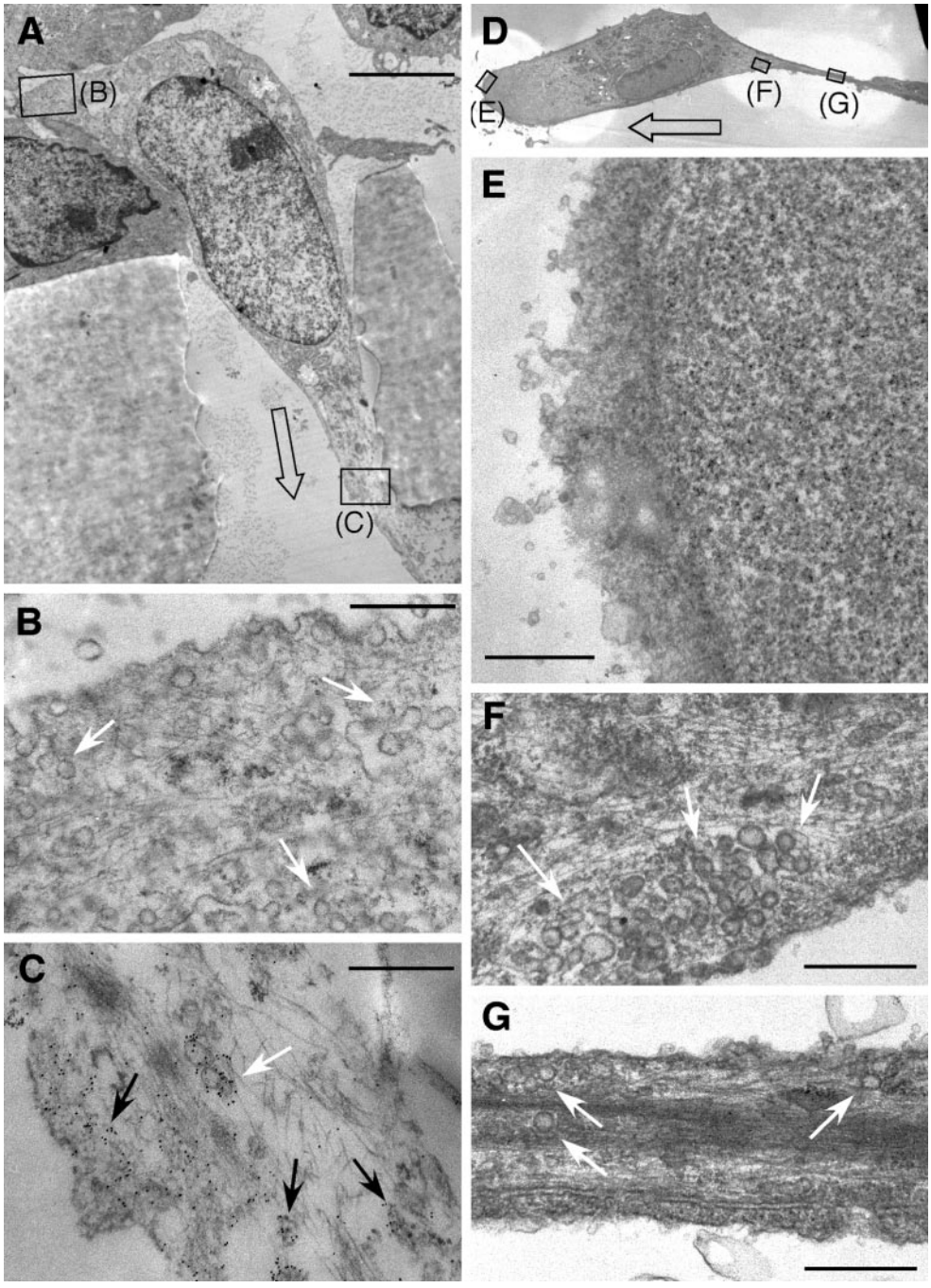

Figure 3. Localization of caveolae in the rear of trans- and planar-migrating ECs. (A) Electron micrograph showing the cross section of an EC transmigrating through the 8-μm pore of a collagen-coated polycarbonate filter. Direction is indicated by open arrow. Caveolin-1 was detected using rabbit anti-caveolin-1 antibody and gold-conjugated goat anti-rabbit IgG (5-nm particles). Enlarged areas are indicated by rectangles. (B) Enlarged view of the cell rear showing abundant caveolae (white arrows). (C) Enlarged view of the forward extension of the cell showing abundant caveolin-1 not associated with membrane or vesicles (black arrows) or associated with caveolae (white arrow). (D) Electron micrographic image of a planar-migrating EC showing a thin-slice parallel and near to the surface of the culture dish. Direction of movement is indicated by open arrow. Enlarged areas are indicated by rectangles. (E) Enlarged view of the cell front containing no detectable caveolae. (F) Enlargement of the rear of the cell body, with abundant caveolae (white arrows). (D) Enlargement of the retracting tail of the cell, also containing caveolae (white arrows). Scale, 3.5 μm (A), 0.4 μm (B and C), and 0.5 μm (E–G).

1995; Isshiki *et al.*, 2002). To determine whether caveolin-1 in transmigrating ECs is transported to the cell front with caveolae, we used electron microscopy to visualize both components, caveolin-1 by antibody labeling and immunogold detection and caveolae by morphology. Ultrathin sections were made in the xz-plane through the center of the pore and the body of the transmigrating cell (Figure 3A). Confirming the results from confocal microscopy, caveolin-1 was abundant in the frontal protrusion of the EC (Figure 3C). The preponderance of the caveolin-1 in the cell front was associated with neither the plasma membrane nor caveolar vesicles but rather was distributed throughout the cytoplasm. In contrast, the cell rear (and top) contained abundant caveolae essentially devoid of caveolin-1 (Figure 3B). These caveolae were typical cave-like structures at the plasma membrane, as well as closed structures, often in groups, below the membrane. Electron microscopy was similarly used to determine the location of caveolae in planar-

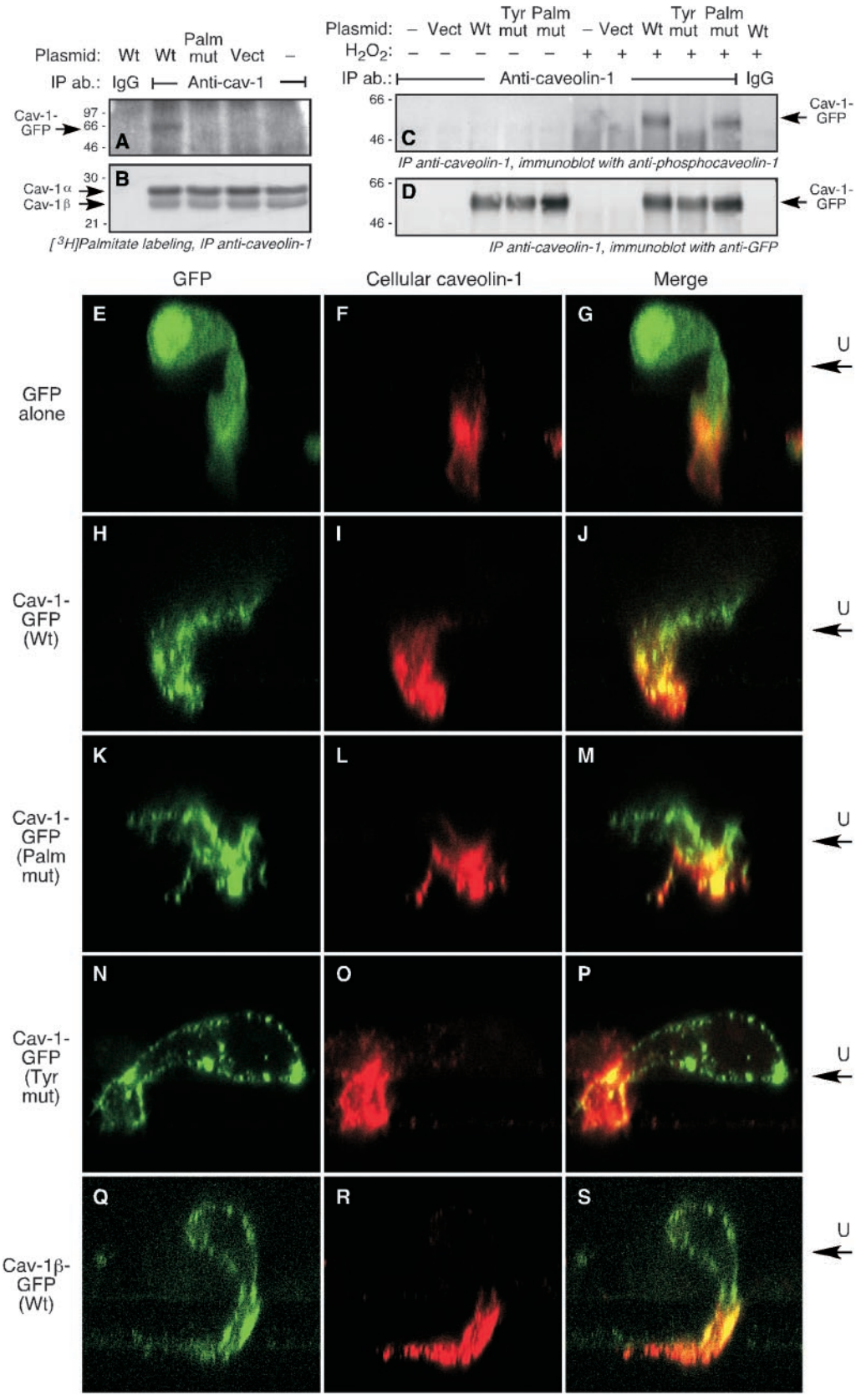
Plasmid: Wt Wt Palm mut Vect –
IP ab.: IgG Anti-cav-1
Cav-1-GFP
97
66
46
A
Cav-1α
Cav-1β
30
21
B
[3H]Palmitate labeling, IP anti-caveolin-1
Plasmid: – Vect Wt Tyr mut Palm mut – Vect Wt Tyr mut Palm mut Wt
H2O2: – – – – – + + + + + +
IP ab.: Anti-caveolin-1 IgG
66
46
C
Cav-1-GFP
IP anti-caveolin-1, immunoblot with anti-phosphocaveolin-1
D
IP anti-caveolin-1, immunoblot with anti-GFP
GFP
Cellular caveolin-1
Merge
GFP alone
Cav-1-GFP (Wt)
Cav-1-GFP (Palm mut)
Cav-1-GFP (Tyr mut)
Cav-1β-GFP (Wt)
E
F
G
H
I
J
K
L
M
N
O
P
Q
R
S
U

Figure 4.

migrating ECs. Thin sections were made in the plane parallel to and very near the dish surface (Figure 3D). The forward lamellipodium was completely devoid of caveolae or any other visible organelles (Figure 3E). In contrast, caveolae were abundant at the rear of the cell body (Figure 3F) and in the retracting tail (Figure 3G). Thus, unlike the differential polarization of caveolin-1 and caveolae in transmigrating ECs, caveolin-1 and caveolae are coordinately polarized during planar migration.

Caveolin-1 Tyr^{14} Is Necessary for Polarization during Transmigration but Not during Planar Migration

We examined whether posttranslational modification of caveolin-1 is required for its polarization during migration. We first tested whether the transfected chimeras were susceptible to posttranslational modification. ECs were transfected with plasmids driving expression of wild-type caveolin-1-GFP, or with GFP-tagged caveolin-1α containing Cys-to-Ser mutations in all three palmitoylation sites (palmitoylation-mutant), or with a Tyr-to-Ala mutation at the Tyr^{14} phosphorylation site (Tyr^{14}-mutant). Wild-type caveolin-1-GFP expressed by ECs was susceptible to acylation as shown by metabolic labeling of the cells with [^{3}H]palmitate and immunoprecipitation with anti-caveolin-1 antibody; as expected, the palmitoylation mutant was not labeled with [^{3}H]palmitate (Figure 4A). Endogenous caveolin-1α and -1β were equally palmitoylated in all of the transfected cells (Figure 4B). To show that transfected caveolin-1-GFP was susceptible to phosphorylation on Tyr^{14}, ECs were treated with H_2O_2 to increase the phosphorylation level (Parat *et al.*, 2002) and phospho-Tyr^{14} was detected by immunoprecipitation of caveolin-1 and immunoblot analysis with anti-phosphocaveolin-1 antibody. Tyr^{14}-phosphorylation was seen in wild-type caveolin-1-GFP but not in the Tyr^{14}-mutant (Figure 4C). The palmitoylation-mutant was also susceptible to phosphorylation. This result was unexpected in view of a report that caveolin-1 palmitoylation was required for its phosphorylation by c-Src (Lee *et al.*, 2001); however, the requirements for phosphorylation in ECs may differ from those in Cos-7 cells cotransfected with caveolin-1 and c-Src. All transfected cells expressed similar levels of caveolin-1-GFP (Figure 4D).

Subconfluent ECs were transfected with a plasmid encoding wild-type or mutated caveolin-1-GFP, or with a control plasmid encoding GFP alone. After recovery, the cells were placed in the upper well of a Boyden chamber and induced to migrate across a polycarbonate filter for 2 h. GFP in transmigrating ECs was visualized by green fluorescence and cellular caveolin-1 by polyclonal anti-caveolin-1 antibody. GFP in ECs transfected with control vector encoding GFP alone was uniformly distributed throughout the cytoplasm (Figure 4E), and it did not colocalize with endogenous caveolin-1, which was primarily located in the forward extension (Figure 4, F and G). Wild-type caveolin-1-GFP substantially colocalized with endogenous caveolin-1 in the leading cellular extension, suggesting that the transfected and cellular proteins undergo similar processing and trafficking (Figure 4, H–J). Essentially identical results were seen with the palmitoylation mutant, indicating that acylation is not required for caveolin-1 polarization in this model (Figure 4, K–M). EC transfected with the Tyr^{14}-mutant of caveolin-1 showed markedly different results. The protein did not show a polarized distribution, but rather was present in discrete patches at or near the plasma membrane, and essentially enveloping the entire cell (Figure 4, N–P). Thus, Tyr^{14} of caveolin-1 is required for its polarization in transmigrating ECs. To confirm this result, ECs were transfected with a construct encoding caveolin-1β-GFP; caveolin-1β lacks the 31 N-terminal amino acids of caveolin-1α, and thus does not contain the Tyr^{14} phosphorylation site of caveolin-1α. Caveolin-1β-GFP did not exhibit any front-to-back polarization but instead was expressed in patches near the plasma membrane and surrounding the entire cell surface (Figure 4, Q–S). This distribution was essentially identical to that of the Tyr^{14}-mutant, confirming the importance of the Tyr^{14} residue for relocalization of caveolin-1 in transmigrating cells.

Similar methods were used to determine whether posttranslational modification of caveolin-1 was also required for the reverse polarization in ECs during planar migration. As described above, in ECs transfected with GFP-containing vector control, GFP was uniformly distributed throughout

Figure 4 (facing page). Polarization of caveolin-1 in transmigrating ECs requires Tyr^{14} phosphorylation but not palmitoylation. (A) ECs were transiently transfected with plasmids encoding C-terminally GFP-tagged wild-type caveolin (Cav)-1 (Wt), C-terminally GFP-tagged caveolin-1 mutated at all three palmitoylation sites (Palm mut), or with the vector (Vect) alone. The cells were subjected to metabolic labeling by incubation with [^{3}H]palmitate for 4 h, and caveolin-1 immunoprecipitated (IP) with rabbit anti-caveolin antibody (ab), or with nonimmune, purified rabbit IgG (IgG) as control. The immunoprecipitate was subjected to SDS-PAGE and fluorography. Radiolabeling of plasmid-driven, Cav-1-GFP was detected by film exposure for 6 mo. (B) [^{3}H]Palmitate labeling of endogenous caveolin-1α and -1β in the same gel was detected by film exposure for 1 mo. (C) ECs were transiently transfected with plasmids encoding C-terminally GFP-tagged caveolin-1 with an Ala substitution at Tyr^{14} (Tyr mut), with wild-type caveolin-1-GFP, with the palmitoylation mutant form of caveolin-1-GFP, or with the vector alone. After recovery, the cells were incubated with medium or with H_2O_2 (5 mM) for 20 min. Caveolin-1 was immunoprecipitated and subjected to SDS-PAGE. Phosphocaveolin-1-GFP was detected by immmunoblot analysis with anti-phosphocaveolin-1 antibody. (D) The amount of caveolin-1-GFP expressed by all transfected cells was shown to be nearly identical by reprobing the immmunoblot shown in C with anti-GFP antibody. (E–G) ECs were transfected with vector encoding GFP and permitted to transmigrate for 2 h across a collagen-coated polycarbonate filter toward 10 ng ml^{-1} basic FGF. The cells were fixed and GFP was visualized by laser-scanning confocal fluorescence analysis (E). The upper face of the filter is indicated as U. Cellular caveolin-1 was detected with rabbit anti-caveolin-1 as primary antibody followed by biotinylated goat anti-rabbit antibody and Texas Red-avidin (F). Overlay of GFP fluorescence and cellular caveolin-1 immunostaining is shown in the merged image (G). (H–J) ECs were transfected with vector encoding wild-type caveolin-1-GFP, and migrating cells were treated and analyzed as in E–G. (K–M) ECs were transfected with vector encoding GFP-tagged caveolin-1 containing Cys-to-Ser mutations in all three palmitoylation sites; migrating cells were treated and analyzed as in E–G. (N–P) ECs were transfected with vector encoding GFP-tagged caveolin-1 containing an Ala substitution at Tyr^{14}; migrating cells were treated and analyzed as in E–G. (Q–S) ECs were transfected with vector encoding GFP-tagged caveolin-1β; migrating cells were treated and analyzed as in E–G.

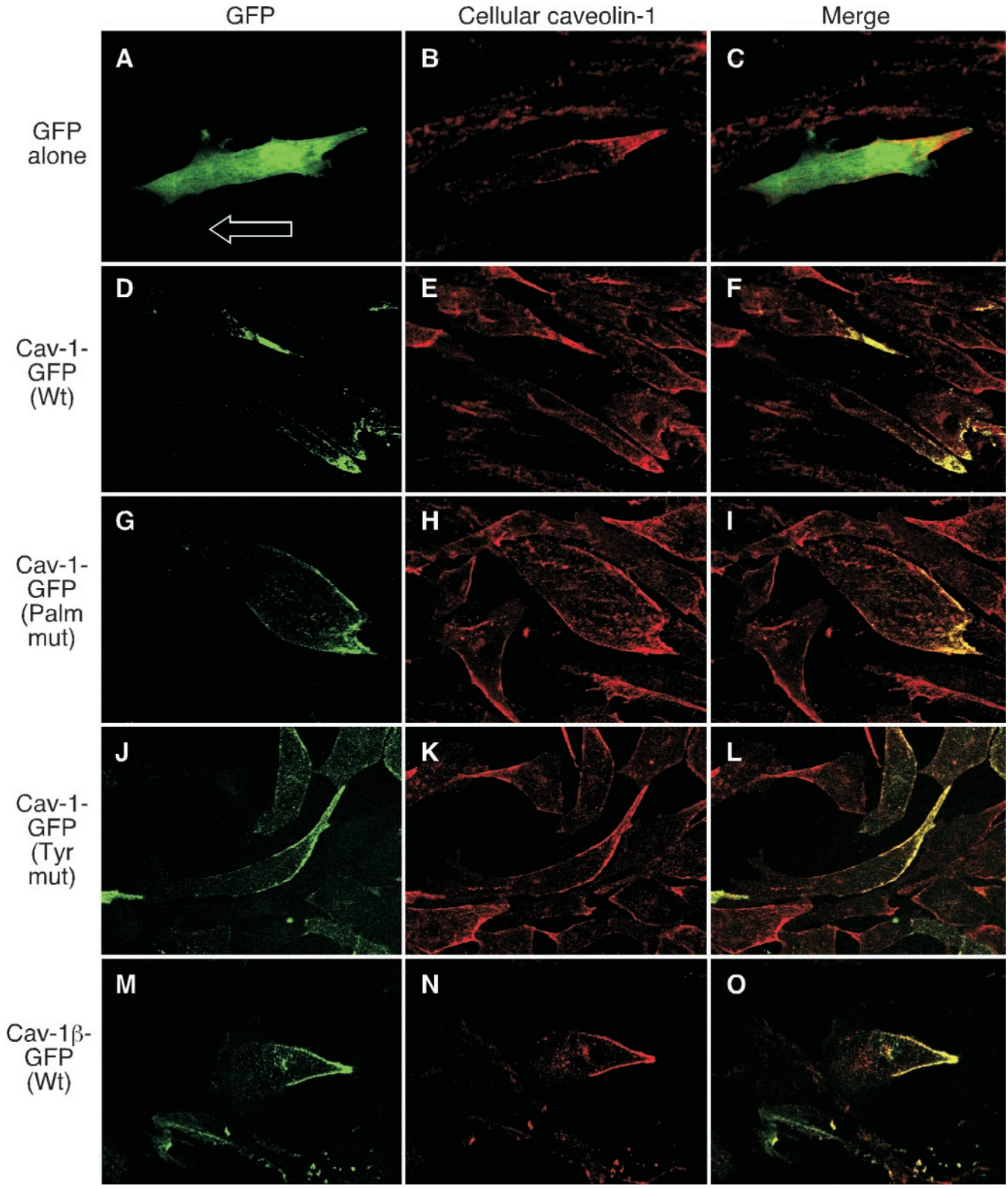
GFP
Cellular caveolin-1
Merge
A
B
C
GFP alone
D
E
F
Cav-1-GFP (Wt)
G
H
I
Cav-1-GFP (Palm mut)
J
K
L
Cav-1-GFP (Tyr mut)
M
N
O
Cav-1β-GFP (Wt)

Figure 5.

the cytoplasm and did not colocalize with cellular caveolin-1, which accumulated in the rear (Figure 5, A–C). In cells expressing wild-type caveolin-1-GFP, the exogenous protein and endogenous caveolin-1 were colocalized in the cell rear (Figure 5, D–F). Likewise, the chimeric palmitoylation mutant and endogenous caveolin-1 also colocalized in ECs (Figure 5, G–I). Interestingly, the Tyr^{14}-mutant colocalized with endogenous caveolin-1, indicating that there is not a requirement for phosphorylation of this amino acid for polarization during planar migration (Figure 5, J–L). Similarly, caveolin-1β-GFP also colocalized with the endogenous caveolin-1 in planar migrating cells (Figure 5, M–O). Thus, the requirement for caveolin-1 Tyr^{14} to establish polarization is unique to the transmigration mode of EC movement in which caveolin-1 translocates to the cell front.

DISCUSSION

We have shown that caveolin-1 and caveolae are polarized in migrating ECs. However, the vector of polarization of caveolin-1 depends on the mode of migration of the cell. Caveolin-1 accumulates in the rear of a planar-migrating cell induced to move by wounding a monolayer, a result in agreement with a previous report (Isshiki *et al.*, 2002). In contrast, caveolin-1 accumulates in the front of a transmigrating cell induced to traverse a filter. In both migration modes, most caveolae accumulate in the cell rear, and caveolin-1 in the front of a transmigrating cell is primarily not associated with caveolae. Our results indicate that modes of cell migration that clearly differ in their morphological characteristics also differ in well-defined biochemical properties. A similar conclusion was made to explain the presence of lipid rafts in the leading edge of insulin growth factor-1–stimulated MCF-7 cells but in the rear of moving T lymphocytes (Mañes *et al.*, 1999; Gómez-Moutón *et al.*, 2001). These authors hypothesized that the difference in polarization is due to the different migration strategies of the two cells: in "crawling" MCF-7 cells, like fibroblasts, the pseudopodia in the leading edge attach tightly to their substrate via integrins and adhesion receptors, whereas the leading edges of "gliding" T cells attach less strongly to the substrate and exhibit fewer integrins and adhesion receptors. Our results differ in that caveolae was found in the rear of both planar- and trans-migrating ECs. However, our finding of differential polarization of caveolin-1 under different conditions in the same cell type, establishes that polarization of the protein, and possibly other motility-related proteins, depends on the mode of migration.

Our results show that transmigrating ECs contain a pool of cytoplasmic caveolin-1 in the forward extension, and a pool of caveolae at the rear of the cell that are essentially devoid of caveolin-1. This result is unexpected given the generally held concept that caveolin-1 is a membrane-bound protein incorporated into caveolae. However, evidence is accumulating for the existence of both soluble caveolin-1 and caveolin-1–deficient caveolae. Soluble caveolin-1 has been observed in the lumen of the endoplasmic reticulum, in secretory vesicles, and in the matrix of mitochondria (Smart *et al.*, 1994; Liu *et al.*, 1999; Li *et al.*, 2001). A soluble, cytoplasmic form has been detected by biochemical (Uittenbogaard *et al.*, 1998) and imaging (Li *et al.*, 2001) methods. A recent model of the intracellular itinerary of caveolin-1 proposes that soluble caveolin-1 is released after its incorporation into caveolae (Liu *et al.*, 2002b). The existence of caveolae without caveolin is more controversial, because caveolin-1 seems to be the structural molecule of the filamentous coat decorating the cytosolic surface of caveolae (Fernandez *et al.*, 2002). In addition, some cells that lack caveolin-1 also lack caveolae, and expression of exogenous caveolin-1 in these cells induces caveolae formation (Fra *et al.*, 1995). However, a recent study suggests that caveolin-1 is not necessary for caveolae invaginations, but rather is a negative regulator of caveolae endocytosis (Le *et al.*, 2002). These authors show that in cells lacking caveolin-1, caveolae endocytosis is so rapid that caveolae cannot be detected by electron microscopy, whereas in cells expressing caveolin-1, the slower rate of endocytosis permits caveolae visualization in thin-section images. They also show that overexpression of a dominant-negative form of dynamin (K44A) slows caveolae internalization and induces caveolar invagination in caveolin- and caveolae-deficient, *abl*-transformed NIH-3T3 cells. These caveolae occur without any concomitant increase in caveolin-1 expression, and they are essentially devoid of immunogold-detectable caveolin-1, in agreement with our finding of caveolin-1–free caveolae at the rear of transmigrating ECs. In view of these results, we propose a model of cell movement in which both caveolae and caveolin-1 accumulate in the rear of planar-migrating cells, and that upon initiation of transmigration, caveolin-1 is released from caveolae and translocates in a soluble form to the cell front (Figure 6).

Transfection of ECs with GFP-tagged caveolin-1 constructs show that caveolin-1β does not translocate to the forward extension of a trans-migrating cell, but rather is retained in plasma membrane patches surrounding the entire cell. Not much is known about the expression or function of caveolin-1β, and in particular, differences between α- and β-isoforms. Insect cell expression of caveolin-1β (or -1α) causes formation of vesicles resembling caveolae by their size, buoyant density, and caveolin-1 enrichment (Li *et al.*, 1996). Similarly, overexpression of caveolin-1β in Chinese hamster ovary cells induces caveolae formation, although less efficiently than the α-isoform (Fujimoto *et al.*, 2000).

Figure 5 (facing page). Polarization of caveolin-1 in planar-migrating ECs requires neither Tyr^{14} phosphorylation nor palmitoylation. (A–C) ECs were transfected with vector encoding GFP and subjected to planar, wound-induced migration for 24 h in the presence of 10 ng ml^{-1} basic FGF. The cells were fixed, and GFP was visualized by confocal fluorescence microscopy (A). Cellular caveolin-1 was detected with rabbit anti-caveolin-1 as primary antibody followed by biotinylated goat anti-rabbit antibody and Texas Red-avidin (B). Overlay of GFP fluorescence and cellular caveolin-1 immunostaining is shown in the merged image (C). (D–F) ECs were transfected with vector encoding wild-type caveolin-1-GFP, and migrating cells were treated and analyzed as in A–C. (G–I) ECs were transfected with vector expressing GFP-tagged caveolin-1 containing Cys-to-Ser mutations in all three palmitoylation sites; migrating cells were treated and analyzed as in A–C. (J–L) ECs were transfected with vector expressing GFP-tagged caveolin-1 containing an Ala substitution at Tyr^{14}; migrating cells were treated and analyzed as in A–C. (M–O) ECs were transfected with vector expressing GFP-tagged caveolin-1-β; migrating cells were treated and analyzed as in A–C.

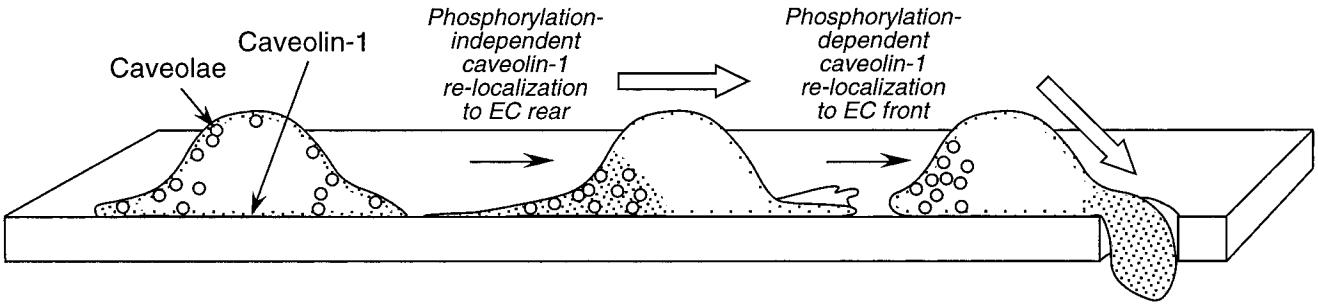

Figure 6. Model showing polarization of caveolin-1 and caveolae in planar- and trans-migrating ECs. Caveolae are indicated by open circles, and caveolin-1 is indicated by dotted regions.

These results suggest the possibility that caveolae in the rear of a transmigrating EC are maintained by the pool of caveolin-1β, which does not translocate to the cell front. Our finding that essentially no immunogold-detectable caveolin-1 remains in the rear of a transmigrating cell seems to contradict this function of caveolin-1β. However, given the relatively weak caveolin-1β signal given by this antibody in denaturing conditions with EC (Parat and Fox, 2001) or fibroblast (Fujimoto *et al.*, 2000) lysates, and the broad distribution of the β-isoform around the entire cell surface, it is possible that the caveolae near the back of transmigrating ECs indeed contain caveolin-1-β, but that it is undetectable in our experiments.

The cellular function of caveolin-1 and caveolae during migration remains unclear, but at least three mechanisms should be considered, namely, effects on the cytoskeleton, signaling, and cholesterol transport. An influence of caveolin-1 on cytoskeletal function is suggested by the binding of caveolin-1 to the actin cross-linking protein filamin and their alignment with Rho-induced stress fibers (Stahlhut and van Deurs, 2000). Caveolin-1 overexpression blocked epidermal growth factor-activated formation of F-actin stress fibers in lamellipodia (Zhang *et al.*, 2000). The apparent localization of phosphocaveolin-1 at focal adhesion sites also suggests an association with the cytoskeleton (Lee *et al.*, 2000; Volonte *et al.*, 2001). Indeed, cytoskeletal disruption potentiates the phosphorylation of caveolin-1 on Tyr^{14} induced by hyperosmotic shock (Volonte *et al.*, 2001), and caveolin-1 depletion causes loss of focal adhesion sites and cell adhesion (Wei *et al.*, 1999). Caveolin-1 may differentially regulate motility-related cytoskeletal components during two- and three-dimensional movement. The well-known role of caveolae and caveolin-1 in compartmentalization and regulation of signaling complexes (Shaul and Anderson, 1998; Smart *et al.*, 1999) suggests that caveolin-1 might influence signal transduction processes involved in cell migration. In support of this hypothesis, polarization of caveolae (in shear-stressed ECs) has been shown to correlate with calcium wave initiation (Isshiki *et al.*, 2002). Moreover, caveolin-1 cofractionates with the Rho family GTPases RhoA Rac1 and Cdc42, although a direct interaction has only been shown for RhoA (Gingras *et al.*, 1998; Michaely *et al.*, 1999). Caveolin-1 copolarizes with the urokinase receptor at the leading edge of migrating smooth muscle cells (Okada *et al.*, 1995), and both may interact with β-1 integrins in a complex that regulates adhesion and signaling through Src-family kinases and focal adhesion kinase (Chapman *et al.*, 1999). It is interesting to speculate that there may be migration mode-specific signaling molecules that are spatially regulated by caveolin. Finally, caveolin-1 and caveolae may regulate cell motility via their ability to transport newly synthesized cholesterol from endoplasmic reticulum to plasma membranes (Smart *et al.*, 1996; Uittenbogaard *et al.*, 1998). Membrane cholesterol may be an important determinant of EC migration because inhibitors of cholesterol synthesis inhibit cell migration (Axel *et al.*, 2000; Vincent *et al.*, 2001), and addition of small amounts of cholesterol to ECs increases migration (Ghosh *et al.*, 2002). Alternatively, caveolae may provide membrane lipids to the expanding forward extension of a moving cell in a manner similar to the proposed polarized delivery of endocytosed clathrin-coated vesicles to the membrane of moving cells (Bretscher and Aguado-Velasco, 1998). The extremely rapid intracellular movement of caveolin-1 and caveolin-1-associated vesicles is consistent with an important role in cell transport processes (Mundy *et al.*, 2002).

Our transfection experiments with caveolin-1 mutants indicate that phosphorylation of caveolin-1 on Tyr^{14} (or possibly the Tyr^{14} residue itself) is required for caveolin-1 accumulation in the leading extension of transmigrating ECs. The mechanism by which caveolin-1 accumulates in this region is not known. A previous report suggests that phosphorylation of Tyr^{14} is required for caveolin-1 binding to Grb7, a Src homology 2-containing adapter protein that regulates cell motility, and for enhanced chemotaxis of 293T cells cotransfected with caveolin-1, c-Src and Grb7 (Lee *et al.*, 2000). It is possible that the interaction with Grb7 may be part of the mechanism driving caveolin-1 to the front of transmigrating cells. In contrast to the requirement for phosphorylation, mutation of all three palmitoylation sites of caveolin-1 did not affect its polarization in transmigrating cells. This was unexpected in view of the requirement of caveolin-1 palmitoylation on Cys^{156} for its interaction with c-Src, and consequently, for c-Src-mediated phosphorylation on Tyr^{14} (Lee *et al.*, 2000; Lee *et al.*, 2001). Possibly, other kinases phosphorylate caveolin-1 in migrating ECs. This hypothesis is supported by our data showing that palmitoylation is not required for H_2O_2-induced phosphorylation, and by a recent report indicating that c-Abl rather than c-Src is responsible for the H_2O_2-induced caveolin-1 phosphorylation (Sanguinetti and Mastick, 2003).

The polarization of caveolin-1 during EC movement suggests that it may have an important role in this process. This

idea is in agreement with recent studies showing that EC caveolin-1 contributes to capillary formation in vivo and in vitro. In several rat tissues examined, phospho-Tyr^{14}-caveolin-1 is most abundant in the endothelium of capillaries and small venules (Aoki *et al.*, 1999). Activators of angiogenesis cause decreased expression of caveolae and caveolin-1 in cultured ECV 304 cells. Antisense-mediated down-regulation of caveolin-1 in ECs reduced capillary tubule formation in vitro and in vivo (Griffoni *et al.*, 2000; Liu *et al.*, 2002a). Likewise, overexpression of caveolin-1 in microvascular ECs increased capillary tubule formation in vitro (Liu *et al.*, 2002a) and intracellular delivery of caveolin-1 scaffolding domain enhanced tube formation (Griffoni *et al.*, 2000). In contrast, exogenous expression of caveolin-1 in caveolin-1-deficient MTLn3 metastatic cells reduced epidermal growth factor-stimulated lamellipodial extension and chemotaxis (Zhang *et al.*, 2000). Future studies of the mechanisms driving caveolae and caveolin-1 polarization may permit the development of reagents that can differentially modulate the migration of ECs in vivo, for example, by inhibiting the EC trans-migration that drives angiogenesis without altering the wound-healing properties of the endothelium.

ACKNOWLEDGMENTS

This work was supported by National Institutes of Health grant HL64357 and National Aeronautics and Space Administration grant 96-HEDS-04 (to P.L.F.) and by an American Heart Association Scientist Development grant (to M.-O.P.).

REFERENCES

Anand-Apte, B., and Fox, P.L. (2002). Tumor angiogenesis. In: Current Clinical Oncology, Melanoma: Biologically Targeted Therapeutics, ed. E.C. Borden, Totowa, NY: Humana Press, 325–360.

Aoki, T., Nomura, R., and Fujimoto, T. (1999). Tyrosine phosphorylation of caveolin-1 in the endothelium. Exp. Cell Res. *253*, 629–636.

Axel, D.I., Riessen, R., Runge, H., Viebahn, R., and Karsch, K.R. (2000). Effects of cerivastatin on human arterial smooth muscle cell proliferation and migration in transfilter cocultures. J. Cardiovasc. Pharmacol. *35*, 619–629.

Bretscher, M.S., and Aguado-Velasco, C. (1998). Membrane traffic during cell locomotion. Curr. Opin. Cell Biol. *10*, 537–541.

Chapman, H.A., Wei, Y., Simon, D.I., and Waltz, D.A. (1999). Role of urokinase receptor and caveolin in regulation of integrin signaling. Thromb. Haemost. *82*, 291–297.

Dietzen, D.J., Hastings, W.R., and Lublin, D.M. (1995). Caveolin is palmitoylated on multiple cysteine residues. Palmitoylation is not necessary for localization of caveolin to caveolae. J. Biol. Chem. *270*, 6838–6842.

Dupree, P., Parton, R.G., Raposo, G., Kurzchalia, T.V., and Simons, K. (1993). Caveolae and sorting in the trans-Golgi network of epithelial cells. EMBO J. *12*, 1597–1605.

Fernandez, I., Ying, Y., Albanesi, J., and Anderson, R.G. (2002). Mechanism of caveolin filament assembly. Proc. Natl. Acad. Sci. USA *99*, 11193–11198.

Fox, P.L., and DiCorleto, P.E. (1984). Regulation of production of a platelet-derived growth factor-like protein by cultured bovine aortic endothelial cells. J. Cell. Physiol. *121*, 298–308.

Fra, A.M., Williamson, E., Simons, K., and Parton, R.G. (1995). De novo formation of caveolae in lymphocytes by expression of VIP21-caveolin. Proc. Natl. Acad. Sci. USA *92*, 8655–8659.

Fujimoto, T., Kogo, H., Nomura, R., and Une, T. (2000). Isoforms of caveolin-1 and caveolar structure. J. Cell Sci. *113*, 3509–3517.

Ghosh, P.K., Vasanji, A., Murugesan, G., Eppell, S.J., Graham, L.M., and Fox, P.L. (2002). Membrane microviscosity regulates endothelial cell motility. Nat. Cell Biol. *4*, 894–900.

Gingras, D., Gauthier, F., Lamy, S., Desrosiers, R.R., and Beliveau, R. (1998). Localization of RhoA GTPase to endothelial caveolae-enriched membrane domains. Biochem. Biophys. Res. Commun. *247*, 888–893.

Gómez-Moutón, C., Abad, J.L., Mira, E., Lacalle, R.A., Gallardo, E., Jimenez-Baranda, S., Illa, I., Bernad, A., Mañes, S., and Martinez, A.C. (2001). Segregation of leading-edge and uropod components into specific lipid rafts during T cell polarization. Proc. Natl. Acad. Sci. USA *98*, 9642–9647.

Griffoni, C., Spisni, E., Santi, S., Riccio, M., Guarnieri, T., and Tomasi, V. (2000). Knockdown of caveolin-1 by antisense oligonucleotides impairs angiogenesis in vitro and in vivo. Biochem. Biophys. Res. Commun. *276*, 756–761.

Haudenschild, C.C., and Schwartz, S.M. (1979). Endothelial regeneration. II. Restitution of endothelial continuity. Lab. Investig. *41*, 407–418.

Isshiki, M., Ando, J., Yamamoto, K., Fujita, T., Ying, Y., and Anderson, R.G. (2002). Sites of Ca^{2+} wave initiation move with caveolae to the trailing edge of migrating cells. J. Cell Sci. *115*, 475–484.

Kolega, J. (1998). Cytoplasmic dynamics of myosin IIA and IIB: spatial 'sorting' of isoforms in locomoting cells. J. Cell Sci. *111*, 2085–2095.

Lawrence, J.B., and Singer, R.H. (1986). Intracellular localization of messenger RNAs for cytoskeletal proteins. Cell *45*, 407–415.

Le, P.U., Guay, G., Altschuler, Y., and Nabi, I.R. (2002). Caveolin-1 is a negative regulator of caveolae-mediated endocytosis to the endoplasmic reticulum. J. Biol. Chem. *277*, 3371–3379.

Lee, H., *et al.* (2000). Constitutive and growth factor-regulated phosphorylation of caveolin-1 occurs at the same site (Tyr-14) *in vivo*: identification of a c-Src/Cav-1/Grb7 signaling cassette. Mol. Endocrinol. *14*, 1750–1775.

Lee, H., Woodman, S.E., Engelman, J.A., Volonte, D., Galbiati, F., Kaufman, H.L., Lublin, D.M., and Lisanti, M.P. (2001). Palmitoylation of caveolin-1 at a single site (Cys-156) controls its coupling to the c-Src tyrosine kinase. Targeting of dually acylated molecules (GPI-linked, transmembrane, or cytoplasmic) to caveolae effectively uncouples c-Src and caveolin-1 (Tyr-14). J. Biol. Chem. *276*, 35150–35158.

Li, S., Song, K.S., Koh, S.S., Kikuchi, A., and Lisanti, M.P. (1996). Baculovirus-based expression of mammalian caveolin in Sf21 insect cells. A model system for the biochemical and morphological study of caveolae biogenesis. J. Biol. Chem. *271*, 28647–28654.

Li, W.P., Liu, P., Pilcher, B.K., and Anderson, R.G. (2001). Cell-specific targeting of caveolin-1 to caveolae, secretory vesicles, cytoplasm or mitochondria. J. Cell Sci. *114*, 1397–1408.

Lisanti, M.P., Scherer, P.E., Vidugiriene, J., Tang, Z., Hermanowski-Vosatka, A., Tu, Y.H., Cook, R.F., and Sargiacomo, M. (1994). Characterization of caveolin-rich membrane domains isolated from an endothelial-rich source: implications for human disease. J. Cell Biol. *126*, 111–126.

Liu, J., Wang, X.B., Park, D.S., and Lisanti, M.P. (2002a). Caveolin-1 expression enhances endothelial capillary tubule formation. J. Biol. Chem. *227*, 10661–10668.

Liu, P., Li, W.P., Machleidt, T., and Anderson, R.G. (1999). Identification of caveolin-1 in lipoprotein particles secreted by exocrine cells. Nat. Cell Biol. *1*, 369–375.

Liu, P., Rudick, M., and Anderson, R.G. (2002b). Multiple functions of caveolin-1. J. Biol. Chem. *277*, 41295–41298.

Mañes, S., Mira, E., Gomez-Mouton, C., Lacalle, R.A., Keller, P., Labrador, J.P., and Martinez, A.C. (1999). Membrane raft microdomains mediate front-rear polarity in migrating cells. EMBO J. *18*, 6211–6220.

Michaely, P.A., Mineo, C., Ying, Y.S., and Anderson, R.G. (1999). Polarized distribution of endogenous Rac1 and RhoA at the cell surface. J. Biol. Chem. *274*, 21430–21436.

Mundy, D.I., Machleidt, T., Ying, Y.S., Anderson, R.G., and Bloom, G.S. (2002). Dual control of caveolar membrane traffic by microtubules and the actin cytoskeleton. J. Cell Sci. *115*, 4327–4339.

Okada, S.S., Tomaszewski, J.E., and Barnathan, E.S. (1995). Migrating vascular smooth muscle cells polarize cell surface urokinase receptors after injury in vitro. Exp. Cell Res. *217*, 180–187.

Parat, M.O., and Fox, P.L. (2001). Palmitoylation of caveolin-1 in endothelial cells is post-translational but irreversible. J. Biol. Chem. *276*, 15776–15782.

Parat, M.O., Stachowicz, R.Z., and Fox, P.L. (2002). Oxidative stress inhibits caveolin-1 palmitoylation and trafficking in endothelial cells. Biochem. J. *361*, 681–688.

Pelkmans, L., Kartenbeck, J., and Helenius, A. (2001). Caveolar endocytosis of simian virus 40 reveals a new two-step vesicular-transport pathway to the ER. Nat. Cell Biol. *3*, 473–483.

Rothberg, K.G., Heuser, J.E., Donzell, W.C., Ying, Y.S., Glenney, J.R., and Anderson, R.G. (1992). Caveolin, a protein component of caveolae membrane coats. Cell *68*, 673–682.

Sanguinetti, A.R., and Mastick, C.C. (2003). c-Abl is required for oxidative stress-induced phosphorylation of caveolin-1 on tyrosine 14. Cell. Signal. *15*, 289–298.

Scherer, P.E., Tang, Z., Chun, M., Sargiacomo, M., Lodish, H.F., and Lisanti, M.P. (1995). Caveolin isoforms differ in their N-terminal protein sequence and subcellular distribution. Identification and epitope mapping of an isoform-specific monoclonal antibody probe. J. Biol. Chem. *270*, 16395–16401.

Schmidt, C.E., Horwitz, A.F., Lauffenburger, D.A., and Sheetz, M.P. (1993). Integrin-cytoskeletal interactions in migrating fibroblasts are dynamic, asymmetric, and regulated. J. Cell Biol. *123*, 977–991.

Schnitzer, J.E., Oh, P., Jacobson, B.S., and Dvorak, A.M. (1995). Caveolae from luminal plasmalemma of rat lung endothelium: microdomains enriched in caveolin, Ca^{2+}-ATPase, and inositol trisphosphate receptor. Proc. Natl. Acad. Sci. USA *92*, 1759–1763.

Shaul, P.W., and Anderson, R.G. (1998). Role of plasmalemmal caveolae in signal transduction. Am. J. Physiol. *275*, L843–L851.

Simionescu, M., Simionescu, N., and Palade, G.E. (1982). Biochemically differentiated microdomains of the cell surface of capillary endothelium. Ann. N.Y. Acad. Sci. *401*, 9–24.

Smart, E.J., Graf, G.A., McNiven, M.A., Sessa, W.C., Engelman, J.A., Scherer, P.E., Okamoto, T., and Lisanti, M.P. (1999). Caveolins, liquid-ordered domains, and signal transduction. Mol. Cell. Biol. *19*, 7289–7304.

Smart, E.J., Ying, Y., Donzell, W.C., and Anderson, R.G. (1996). A role for caveolin in transport of cholesterol from endoplasmic reticulum to plasma membrane. J. Biol. Chem. *271*, 29427–29435.

Smart, E.J., Ying, Y.S., Conrad, P.A., and Anderson, R.G. (1994). Caveolin moves from caveolae to the Golgi apparatus in response to cholesterol oxidation. J. Cell Biol. *127*, 1185–1197.

Stahlhut, M., and van Deurs, B. (2000). Identification of filamin as a novel ligand for caveolin-1: evidence for the organization of caveolin-1-associated membrane domains by the actin cytoskeleton. Mol. Biol. Cell *11*, 325–337.

Uittenbogaard, A., and Smart, E.J. (2000). Palmitoylation of caveolin-1 is required for cholesterol binding, chaperone complex formation, and rapid transport of cholesterol to caveolae. J. Biol. Chem. *275*, 25595–25599.

Uittenbogaard, A., Ying, Y., and Smart, E.J. (1998). Characterization of a cytosolic heat-shock protein-caveolin chaperone complex. Involvement in cholesterol trafficking. J. Biol. Chem. *273*, 6525–6532.

Vincent, L., Chen, W., Hong, L., Mirshahi, F., Mishal, Z., Mirshahi-Khorassani, T., Vannier, J.P., Soria, J., and Soria, C. (2001). Inhibition of endothelial cell migration by cerivastatin, an HMG-CoA reductase inhibitor: contribution to its anti-angiogenic effect. FEBS Lett. *495*, 159–166.

Volonte, D., Galbiati, F., Pestell, R.G., and Lisanti, M.P. (2001). Cellular stress induces the tyrosine phosphorylation of caveolin-1 (Tyr^{14}) via activation of p38 mitogen-activated protein kinase and c-Src kinase. Evidence for caveolae, the actin cytoskeleton, and focal adhesions as mechanical sensors of osmotic stress. J. Biol. Chem. *276*, 8094–8103.

Wei, Y., Yang, X., Liu, Q., Wilkins, J.A., and Chapman, H.A. (1999). A role for caveolin and the urokinase receptor in integrin-mediated adhesion and signaling. J. Cell Biol. *144*, 1285–1294.

Zhang, W., Razani, B., Altschuler, Y., Bouzahzah, B., Mostov, K.E., Pestell, R.G., and Lisanti, M.P. (2000). Caveolin-1 inhibits epidermal growth factor-stimulated lamellipod extension and cell migration in metastatic mammary adenocarcinoma cells (MTLn3). Transformation suppressor effects of adenovirus-mediated gene delivery of caveolin-1. J. Biol. Chem. *275*, 20717–20725.